ICSV13 - Vienna
The Thirteenth International Congress on Sound and Vibration
Vienna, Austria, July 2-6, 2006

CAN GRINDING BE CHAOTIC?

Nicolae–Doru Stănescu*[1], Marina Pandrea[1], and Claude Fressengeas[2]

[1]University of Piteşti, Department of Applied Mechanics
Târgu din Vale, 1, 110040, Piteşti, Romania
[2]Laboratoire de Physique et Mécanique des Matériaux,
Université de Metz-CNRS, Ile du Saulcy, 57045 Metz Cedex 01, France
s_doru@yahoo.com

Abstract
This paper presents a non-linear model for the external grinding of a cylindrical work-piece. A system of non-linear differential equations for the vibrations of the tool and the work-piece is obtained. Non-linearity comes from the cutting force dependence on the feeding velocity and depth of cut. Results of simulation are discussed. A chaotic regime is found for realistic values of the grinding parameters.

INTRODUCTION

The accuracy of the ground surfaces is a major concern in grinding processes. The non-uniformity of these surfaces is considered to stem from vibrations arising from the interactions of the tool-work-piece-machine system. This interaction is non-linear due to expressions of the cutting force as a function of the feeding velocity and depth of cut. It is the aim of this paper to investigate the consequences of these non-linearities on the dynamics of the system. In particular we shall examine the possibility of chaotic motions of the tool and work-piece, as might be expected from the nature of the self-excited oscillations the system encounters.

There are two approaches to the understanding of the system dynamics. The direct method consists in modelling this dynamics, whereas the inverse method aims at analysing the experimental time series in order to deduce the nature of the underlying dynamics. Here, we shall model the grinding system, including the work-piece, in order to determine if a chaotic regime can be found. In previous models, only the vibrations of the tool were considered. However, experiments show that the vibrations of the work-piece are of importance for the accuracy of the ground surface. In our model, the tool has two degrees of freedom, while the work-piece has also one degree of freedom, orthogonal to the feeding velocity. The resulting differential equations of motion are coupled through the expression of the cutting force.

A MODEL FOR ORTHOGONAL GRINDING

We consider an orthogonal grinding machine where the cutting edge is parallel to the work-piece surface and normal to the cutting direction (see Fig. 1). We assume that the depth of cut, denoted by w is much smaller than the cutting width. The tool and the work-piece have rotational motions with angular speed ω_t and ω_w, respectively. In what follows, the indexes t and w refer to the grinding wheel and to the work-piece respectively. In Fig. 1(a) w_s denotes the pre-set value for the depth of cut. The work-piece, considered homogeneous and infinitely long in the z-direction, moves in this direction with velocity v_{fs}. v_{fs} and v_w denote the pre-set values for the feeding speed and the tangential velocity of the work-piece, respectively. Due to the cutting force the tool is deformed. Its visco-elastic and inertial properties are described by a two degrees of freedom oscillator, which is presented in Fig. 1(b). We assume that the work-piece also vibrates, but only in the y-axis direction. Its visco-elastic and inertial properties are therefore described by a one-degree of freedom oscillator, shown in Fig. 1(c).

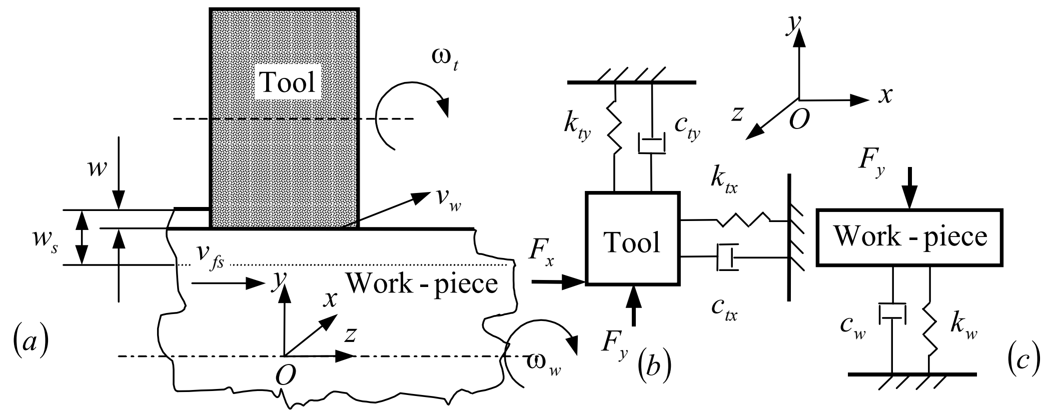

Figure 1 – A model for orthogonal grinding

The state variables of the process are the displacement of the cutting edge in the (x, y) directions and of the work-piece in the y direction (x_t, y_t, y_w). The dynamics of these state variables is given by the following differential equations:

$$m_t\ddot{x}_t + c_{tx}\dot{x}_t + k_{tx}x_t = F_x;\ m_t\ddot{y}_t + c_{ty}\dot{y}_t + k_{ty}y_t = F_y;\ m_w\ddot{y}_w + c_w\dot{y}_w + k_w y_w = -F_y. \quad (1)$$

The friction velocity in the direction of the y-axis is given by $v_f = \frac{v}{R}$, where R is a factor due to plastic shear deformation, which value is $R = R_0\left[C_4\left(\frac{v}{v_0} - 1\right)^2 + 1\right]$.

In addition, the following instantaneous relations are satisfied: $w(t) = w_s - y_t(t) + y_w(t)$, $v(t) = v_w - \dot{x}_t(t)$, $v_f(t) = \dfrac{v(t)}{R(t)} - \dot{y}_t(t) + \dot{y}_w(t)$.

In Equations (1) we assume that the inertial mass of the tool is the same for both directions x and y. The dependence between the components F_x and F_y of the cutting force is expressed by $F_y = K_F \cdot F_x$, where K_F is a friction coefficient. According to the experimental data, the component F_x of the cutting force is of the form

$$F_x \propto w^{0.6}. \tag{2}$$

Using that dependence on the depth of cut, and otherwise following Grabec for the dependence on the velocity v, the expressions of the cutting force F_x, and friction coefficient K_F are then taken as:

$$F_x = F_{x_0}\left(\frac{w}{w_0}\right)^{0.6}\left[C_1\left(\frac{v}{v_0}-1\right)^2+1\right]\Theta(w)\Theta(v), \tag{3}$$

$$K_F = K_{F_0}\left[C_2\left(\frac{v_w}{v_0}-1\right)^2+1\right]\cdot\left[C_3\left(\frac{w}{w_0}-1\right)^2+1\right]\Theta(F_x)\operatorname{sgn}(v_f), \tag{4}$$

where Θ is the Heaviside function and sgn is the sign function. The parameters F_{x_0}, w_0, v_0, K_{F_0}, C_1, C_2, C_3, C_4, R_0 denote specific cutting conditions. Due to the exponent 0.6 in relation (2), the present model exhibits a higher non-linearity than the previous models.

DIMENSIONLESS SYSTEM

We shall introduce the non-dimensional time as $T = t\dfrac{v_0}{w_0} = t\omega_0$. Using the dimensionless variables: $X_t = \dfrac{x_t}{w_0}$, $Y_t = \dfrac{y_t}{w_0}$, $Y_w = \dfrac{y_w}{w_0}$, $V_w = \dfrac{v_w}{v_0}$, $V = V_w - X_t'$, $W_S = \dfrac{w_s}{w_0}$, $W = W_s - Y_t + Y_w$, and the notations: $C_{tx} = \dfrac{c_{tx}w_0}{m_t v_0} = \dfrac{c_{tx}}{m_t\omega_0}$, $K_{tx} = \dfrac{k_{tx}w_0^2}{m_t v_0^2} = \dfrac{k_{tx}}{m_t\omega_0^2}$, and similar, $F_0 = \dfrac{F_{x_0}}{m_t\omega_0^2 w_0}$, $F_1 = \dfrac{F_{x0}}{m_w\omega_0^2 w_0^{0.6}} = F_0\dfrac{m_t}{m_w} = \lambda F_0$,
$F = F_0 W^{0.6}\left[C_1(V-1)^2+1\right]\Theta(W)\Theta(V)$, $F_w = F_1 W^{0.6}\left[C_1(V-1)^2+1\right]\Theta(W)\Theta(V)$,
$R = R_0\left[C_4(V-1)^2+1\right]$, $K_F = K_{F_0}\left[C_2(V_f-1)^2+1\right]\left[C_3(W-1)^2+1\right]\operatorname{sgn}(V_f)\Theta(F)$,
$V_f = V - RY_t' + RY_w'$, $X_t = Z_1$, $X_t' = Z_2$, $Y_t = Z_3$, $Y_t' = Z_4$, $Y_w = Z_5$, $Y_w' = Z_6$, we obtain from the previous equations the non-dimensional system:

$$\frac{\mathrm{d}Z_1}{\mathrm{d}T} = Z_2\,;\ \frac{\mathrm{d}Z_3}{\mathrm{d}T} = Z_4\,;\ \frac{\mathrm{d}Z_5}{\mathrm{d}T} = Z_6\,;$$

$$\begin{aligned}
\frac{\mathrm{d}Z_2}{\mathrm{d}T} &= -C_{tx}Z_2 - K_{tx}Z_1 + F_0(W_s - Z_3 + Z_5)^{0.6}\left[C_1(V_w - Z_2 - 1)^2 + 1\right]\Theta(W)\Theta(V);\\
\frac{\mathrm{d}Z_4}{\mathrm{d}T} &= -C_{ty}Z_4 - K_{ty}Z_3 + K_{F_0}F_0(W_s - Z_3 + Z_5)^{0.6}\left[C_1(V_w - Z_2 - 1)^2 + 1\right]\times\\
&\times\left\{C_2\left\{V_w - Z_2 + R_0\left[C_4(V_w - Z_2 - 1)^2 + 1\right](-Z_4 + Z_6) - 1\right\}^2 + 1\right\}\times\\
&\times\left[C_3(W_s - Z_3 + Z_5 - 1)^2 + 1\right]\Theta(W)\Theta(V)\Theta(F)\operatorname{sgn}(V_f);\\
\frac{\mathrm{d}Z_6}{\mathrm{d}T} &= -C_wZ_6 - K_wZ_5 - \lambda K_{F_0}F_0(W_s - Z_3 + Z_5)^{0.6}\left[C_1(V_w - Z_2 - 1)^2 + 1\right]\times\\
&\times\left\{C_2\left\{V_w - Z_2 + R_0\left[C_4(V_w - Z_2 - 1)^2 + 1\right](-Z_4 + Z_6) - 1\right\}^2 + 1\right\}\times\\
&\times\left[C_3(W_s - Z_3 + Z_5 - 1)^2 + 1\right]\Theta(W)\Theta(V)\Theta(F)\operatorname{sgn}(V_f).
\end{aligned} \tag{5}$$

In the next section, this system will be solved using a fourth-order Runge-Kutta method.

SYSTEM SOLUTION

Number Of Critical Points

In this paragraph we consider the Heaviside and sign functions to be $\Theta = 1$ and $\operatorname{sgn} = 1$. The critical points of the system (5) are obtained by equating the right hand side terms of the system to zero. The first, second and third equation provide immediately the values: $Z_2 = 0$, $Z_4 = 0$, $Z_6 = 0$, which, replaced in the rest of the equations, lead to:

$$K_{tx}Z_1 + F_0(W_s - Z_3 + Z_5)^{0.6}\left[C_1(V_w - 1)^2 + 1\right] = 0\,, \tag{6-1}$$

$$\begin{aligned}
&-K_{ty}Z_3 + K_{F_0}F_0(W_s - Z_3 + Z_5)^{0.6}\left[C_1(V_w - 1)^2 + 1\right]\times\\
&\times\left[C_2(V_w - 1)^2 + 1\right]\left[C_3(W_s - Z_3 + Z_5 - 1)^2 + 1\right] = 0\,,
\end{aligned} \tag{6-2}$$

$$\begin{aligned}
&-K_wZ_5 - \lambda K_{F_0}F_0(W_s - Z_3 + Z_5)^{0.6}\left[C_1(V_w - 1)^2 + 1\right]\times\\
&\times\left[C_2(V_w - 1)^2 + 1\right]\left[C_3(W_s - Z_3 + Z_5 - 1)^2 + 1\right] = 0\,.
\end{aligned} \tag{6-3}$$

In these conditions, when $\Theta = 1$ and $\operatorname{sgn} = 1$, the inequation $Z_3 - Z_5 < W_s$ is always satisfied. From the last two relations of the system (6) we now obtain $Z_5 = -\lambda\frac{K_{ty}}{K_w}Z_3 = \psi Z_3$, with $\psi < 0$. The second relation of the system (6) can thus be written

$$\begin{aligned}
K_{ty}Z_3 &= K_{F_0}F_0(W_s - Z_3 + \psi Z_3)^{0.6}\left[C_1(V_w - 1)^2 + 1\right]\times\\
&\times\left[C_2(V_w - 1)^2 + 1\right]\left[C_3(W_s - Z_3 + \psi Z_3 - 1)^2 + 1\right].
\end{aligned} \tag{7}$$

In the working interval $\left(0, \frac{W_s}{1-\psi}\right)$, the left hand side term is a strictly increasing linear function, while the right hand side term is a strictly decreasing function. In these conditions the equation (7), considered as an equation for the variable Z_3, has one and only one solution. Therefore, there is also one solution for Z_1 and Z_5 and only one critical point.

Following references, the working parameters are as follows: $C_{tx} = 0$, $C_{ty} = 0$, $C_w = 0$, $K_{tx} = 1$, $K_{ty} = 0.25$, $K_w = 0.9$, $\lambda = 1$, $F_0 = 0.5$, $C_1 = 0.3$, $C_2 = 0.7$, $C_3 = 1.5$, $C_4 = 1.2$, $K_{F_0} = 0.36$, $R_0 = 2.2$. We shall consider two cases based on typical experimental data. The first case is characterised by $W_s = 0.4$, $V_w = 1.31$, and the second one by $W_s = 1.2$, $V_w = 1.38$. For these values, instabilities for the motions of the tool-work-piece system were observed. For the first considered case one finds the following values for the critical point co-ordinates: $Z_1 = 0.07671$, $Z_3 = 0.28022$, $Z_5 = -0.07784$; for the second case the critical point is given by: $Z_1 = 0.25619$, $Z_3 = 0.69989$, $Z_5 = -0.19441$. A standard linear stability analysis of this critical point leads to the characteristic equation

$$\lambda^6 + 0.58544\lambda^5 + 2.29853\lambda^4 + 0.84301\lambda^3 + 1.55931\lambda^2 + 0.25414\lambda + 0.28187 = 0 \quad (8)$$

for the first case. In the second case the characteristic equation is

$$\lambda^6 + 0.49244\lambda^5 + 2.43827\lambda^4 + 0.70483\lambda^3 + 1.80460\lambda^2 + 0.20105\lambda + 0.36707 = 0, \quad (9)$$

where λ is the complex rate of growth of the perturbation. It was checked that in both cases the six order determinant for the Routh-Hurwitz criterion has negative values. Thus, the critical point is unstable in the linear approximation, and it is therefore unstable in the original system.

Numerical Analysis

Due to the complex form of the system (5) a numerical solution is looked for. The working parameters are described in the previous section. In addition, we consider $\Delta T = 0.025$, $N_{iter} = 1.6 \times 10^4$. The initial conditions are: $Z_1 = 0.6$, $Z_2 = 0.3$, $Z_3 = 0$, $Z_4 = 0$, $Z_5 = 0$, $Z_6 = 0$.

One can observe the existence of a transient regime in the studied cases (see Fig. 2, a). A clear transition exists between this regime and the rest of the time series. The situation is quite different for different variables, i. e. the route to the second regime and its length differ from variable to variable. Beyond the transient regime, the time series presents irregularity and looks random. In our study we have a six-dimension phase space. We represent projections on two dimensions of this space (see Fig. 2, b). A characteristic of chaotic motion is that its portrait in the phase space is defined by a non-closed curve which occupies a well-defined zone. This characteristic appears very clearly in the figures, which show both linear instability and global stability of the critical point. The non-linearity of the cutting force is clearly seen in Fig. 3. It has two reasons: the first one is its dependence on the depth of cut. The second is the use of the Heaviside function to represent the loss of contact between the tool and the work-piece. The reader can observe that there is no rule for the determination of the period when the tool is in contact with the work-piece and when it is not. This variation of the cutting force is at the origin of the waving form of the work-piece surface.

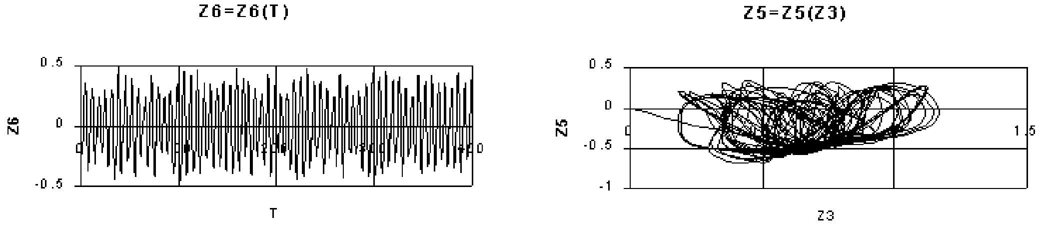

a) b)

Figure 2 – a) Variation of Z_6 versus T for the second case. One can observe a period of transition for T between 0 and 25 time units; b) Variation of Z_5 versus Z_3 for the second case. Initial conditions are $Z_1 = 0.26$, $Z_2 = 0$, $Z_3 = 0.70$, $Z_4 = 0$, $Z_5 = -0.2$, $Z_6 = 0$. The critical point is at $Z_1 = 0.25619$, $Z_3 = 0.69989$, $Z_5 = -0.19441$. The reader can easy see the instability of the critical point, as well as its global stability

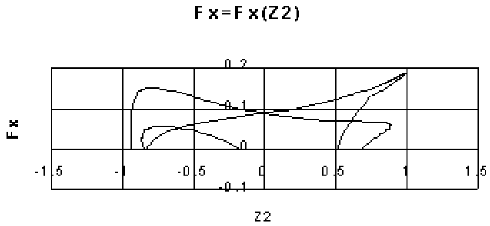

Figure 3 – Variation of the force F_x versus Z_2 in the first case. One can observe the cross points and zone where the force is null (i. e. the tool looses the contact with the work-piece). Time T was elected between 100 and 300 time units

The reader is now asked to refer to Fig. 4, a showing the entropy of the system. The entropy is a measure of the disorder degree in the system. It is clear from Fig. 4, a that the entropy has large values, which is a property of a chaotic system, among others. One can observe that the power spectra are continuous with broad-band basis and peaks (see Fig. 4, b) due to the periodical components of the flow. This aspect of the power spectra is also compatible with chaos. The Lyapunov exponents are calculated as functions of F_0 and W_s (see Fig. 5). It is known that a chaotic system is characterised by at least one positive Lyapunov exponent, the sum of Lyapunov exponents being negative. We have one well defined positive exponent (for the variable Z_1, see Fig. 5, a) and the sum of Lyapunov exponents is negative. The convergence of all the above results is a clear indication that the dynamics is indeed chaotic. Referring now to the Fig. 5, b and c one can see that if the Lyapunov exponent for the variable Z_1 (this variable is the displacement in the x-direction) increases, the Lyapunov exponent for the variable Z_2 (the velocity in the x-

direction) decreases when the depth of cut W_s increases. This phenomenon is indicative of the transformation of the energy input into potential energy (given by displacement) or in kinetic energy (given by velocity). For this reason we believe that the Lyapunov exponents can be considered a measure of the transformation of energy.

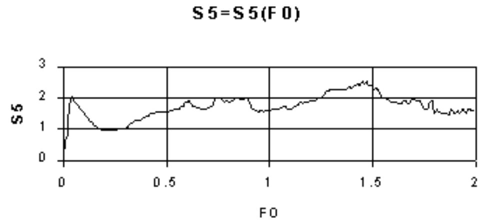

a)

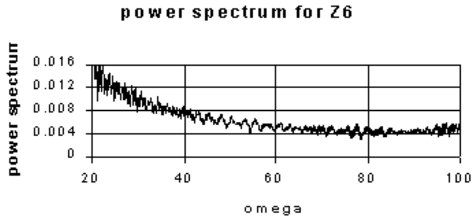

b)

Figure 4 – a) Variation of the entropy for the variable Z_5 versus F_0 in the second case; b) Power spectrum for the variable Z_6 in the second case

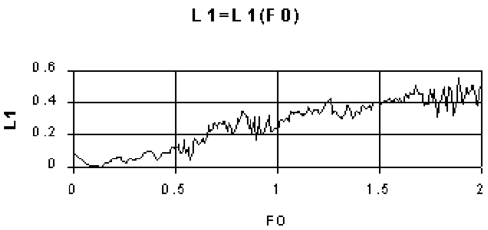

a)

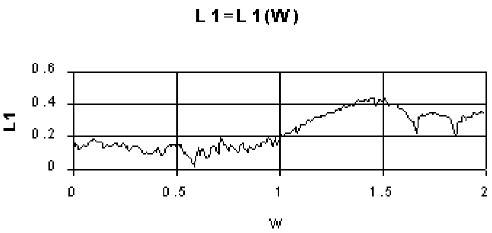

b)

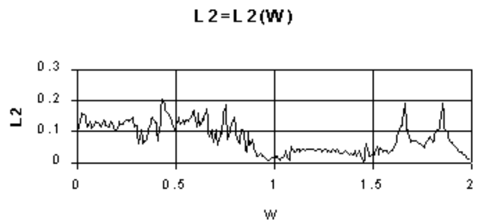

c)

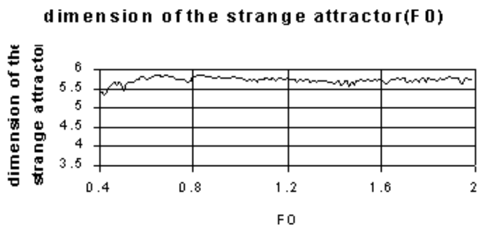

d)

Figure 5 – a) Lyapunov exponent for Z_1 versus F_0. In this case $W_s = 0.4$ and $V_w = 1.31$. The reader can observe that this Lyapunov exponent is positive; b) Lyapunov exponent for Z_1 versus W_s. In this case $F_0 = 0.5$ and $V_w = 1.38$. The reader can see that this Lyapunov exponent is positive; c) Lyapunov exponent for Z_2 versus W_s. In this case $F_0 = 0.5$ and $V_w = 1.38$. The reader can see that this Lyapunov exponent is positive; d) Dimension of the strange attractor versus F_0 in the first case. One can see that this dimension is between 5.3 and 5.9

The Lyapunov dimension of the strange attractor is calculated by using the Kaplan-Yorke conjecture. For our model we found the dimension of the strange attractor to be between 5.3 and 5.9 (see Fig. 5, d). This value proves that all six variables are needed to describe the chaotic dynamics of the system and that there is no reduction in the number of variables. In Grabec's model (which considered only four variables) the dimension of strange attractor was found between 2.4 and 2.7. In addition, the dimension of the strange attractor implies that previous models did not capture all the dynamics.

All the results presented above lead to the conclusion that there exists a chaotic regime in the grinding processes. Our model considers the interaction between the work-piece and the rest of the system, which is a new approach in comparison with the previous models. We also found different regimes for the transformation of energy (kinetic, elastic) inside the chaotic region.

CONCLUSIONS

In our paper we presented a non-linear model with three degrees of freedom for the external cylindrical grinding. We considered the vibrations of the tool in two directions and the vibrations of the work-piece in one direction. The instability of the cutting process stems from three factors: the dependence of the cutting force on the feeding velocity and the depth of cut, and the dependence of the friction coefficient on the friction velocity. We proved the existence of one critical point and its linear instability. We also proved unambiguously the existence of chaos from the clear convergence of indications from various methods of different nature. Furthermore, different regimes for the transformation of the input energy were found in the chaotic region, either in elastic energy or in kinetic energy, depending on the depth of cut. The question arises of what is the number of relevant variables in order to describe the chaotic dynamics of the system when the model includes a high number of degrees of freedom, or in other words, if there is a significant reduction in the number of variables in such models. This will be the object of future work.

REFERENCES

H. E. Merrit, “Theory of self-excited machine-tool chatter, Contribution of machine-tool chatter research-1”, Transactions of ASME, Journal of Engineering for Industry, **87(4)**, 447-454 (1965).

S. A. Tobias, *Machine-Tool Vibrations*. (Blackall, London, 1965).

J. Tlusty, “Machine Dynamics” in R. I. King (Ed.) *Handbook of High Speed Machining Technology*, (Chapman and Hall, New-York, 1985).

H. D. I. Abarbanel, *Analysis of Observed Chaotic Data.* (Springer-Verlag, New York, 1996).

I. Grabec, “Chaos generated by the cutting process”, Physics Letters A, vol. **117**, no. 8, 384-386 (1986).

I. Grabec, “Chaotic dynamics of the cutting process” International Journal of Machine Tools & Manufacture **28**, 2179–2185 (1988).

P. Potočnik, I. Grabec., “Non-linear model predictive control of a cutting process” Neurocomputing **43**, 107–126 (2002).

C. Picoş, O. Pruteanu, C. Bohosievici, Gh. Coman, V. Braha, D. Paraschiv, L. Slătineanu, T. Grămescu, A Marin, V Ionesii, A. Toca, *Proiectarea Tehnologiilor de Prelucrare Mecanică prin Aşchiere*, (Universitas, Chişinău, 1992) (in Romanian).

R. F. Gans, “When is cutting chaotic”, Journal of Sound and Vibration, **188(1)**, 75-83 (1995).

J. L. Kaplan, J. A. Yorke, in: H. O. Peitgen and H. O. Walther (Ed.), *Functional Differential Equations and Approximation of Fixed Points*. (Springer, Berlin, 204, 1979).

P. Lipinski, O. Sinot, A. Lefebvre, “Private communication”.